Improving the Performance of Solar Cells Under Non-Perpendicular Incidence by Photonic Crystal

Xiansheng Tang, Ziguang Ma, Wenqi Wang, Zhen Deng, Yang Jiang, Wenxin Wang, Hong Chen, Na Zhang, Kaiyun Huang, Chunhua Du, and Haiqiang Jia

***Abstract*—Photonic crystal has been proved to manipulate light effectively and improve the performance of solar cells. In this paper, high-performance GaAs-based solar cells with photonic crystal were fabricated to decrease the dependence on the angle of incident light. Photoluminescence (PL) intensity of solar cells with photonic crystal reduced only 8% when the incident angle changed from 10° to 30°, while the PL intensity of the ordinary solar cells decreased 39% under the same condition. It manifests the photonic crystal can manipulate the incident light in turn reduce the dependence of incident light angle. Besides, the short circuit current of solar cells was increased by 32% after the photonic crystal was added. When the incident angle of light increased to 30° from 0°, the short circuit current of ordinary solar cell decreased 29.5%, while that of solar cell with photonic crystals reduced 12%. Correspondingly, the photoelectric conversion efficiency (PCE) of ordinary solar cells was reduced 31.2%. In contrast, solar cells with photonic crystal decreased only 11.5%. The enhancement factor of the PCE of solar cells with photonic crystal to that of ordinary solar cells increases from 1.26 to 1.6 as the incident angle rises to 30°from 0°. In summary, solar cells with photonic crystal are less sensitive to the incident angle and could absorb more light without angle limits, then increase the PCE. These solar cells with photonic crystals are promising in low-cost and high power conversion efficiency solar cell fields.**

***Index Terms*—Solar cells, photonic crystal, photoelectric conversion efficiency.**

Manuscript received June 22, 2021; accepted July 11, 2021. Date of publication July 14, 2021; date of current version August 3, 2021. This work was supported in part by the National Natural Science Foundation of China under Grants 61804176, 61991441, and 62004218, in part by the Strategic Priority Research Program of Chinese Academy of Sciences under Grant XDB01000000, in part by Youth Innovation Promotion Association CAS, and in part by the Education and Teaching Reform Foundation of TangShan Normal University under Grant 2018001029. *(Corresponding author: Yang Gao.)*

Xiansheng Tang is with the Key Laboratory for Renewable Energy, Beijing Key Laboratory for New Energy Materials and Devices, Beijing National Laboratory for Condensed Matter Physics, Institute of Physics, Chinese Academy of Science, Beijing 100190, China, with the University of Chinese Academy of Sciences, Beijing 100049, China, and also with the Center of Material and Optoelectronics Engineering, University of Academy of Science, Beijing 100049, China (e-mail: 18811681359@163.com).

Ziguang Ma and Yang Jiang are with the Key Laboratory for Renewable Energy, Beijing Key Laboratory for New Energy Materials and Devices, Beijing National Laboratory for Condensed Matter Physics, Institute of Physics, Chinese Academy of Science, Beijing 100190, China, and also with the Center of Material and Optoelectronics Engineering, University of Academy of Science, Beijing 100049, China (e-mail: zgma@iphy.ac.cn; jiangyang@iphy.ac.cn).

Wenqi Wang is with the Key Laboratory for Renewable Energy, Beijing Key Laboratory for New Energy Materials and Devices, Beijing National Laboratory for Condensed Matter Physics, Institute of Physics, Chinese Academy of Science, Beijing 100190, China (e-mail: wenqi_wang@iphy.ac.cn).

Zhen Deng and Chunhua Du are with the Key Laboratory for Renewable Energy, Beijing Key Laboratory for New Energy Materials and Devices, Beijing National Laboratory for Condensed Matter Physics, Institute of Physics,Chinese Academy of Science, Beijing 100190, China, with the Center of Material and Optoelectronics Engineering, University of Academy of Science, Beijing 100049, China, and also with the Yangtze River Delta Physics Research Center, Liyang, Jiangsu 213000, China (e-mail: zhen.deng@iphy.ac.cn; duchunhua@iphy.ac.cn).

Wenxin Wang, Hong Chen, and Haiqiang Jia are with the Key Laboratory for Renewable Energy, Beijing Key Laboratory for New Energy Materials and Devices, Beijing National Laboratory for Condensed Matter Physics, Institute of Physics, Chinese Academy of Science, Beijing 100190, China, with the Center of Material and Optoelectronics Engineering, University of Academy of Science, Beijing 100049, China, and also with the Songshan Lake Material Laboratory, Dongguan, Guangdong 523808, China (e-mail: wxwang@iphy.ac.cn; hchen@iphy.ac.cn; mbe2@iphy.ac.cn).

Na Zhang is with the State Key Laboratory of Artificial Microstructure and Mesoscopic Physics, School of Physics, Peking University, Beijing 100871, China (e-mail: zhangna0730@pku.edu.cn).

Kaiyun Huang is with the College of Physics Science and Technology, Tangshan Normal University, Tangshan 063000, China (e-mail: 18366111512@163.com).

Digital Object Identifier 10.1109/JPHOT.2021.3097070

I. Introduction

SOLAR energy, one of the most important energy sources in the future, is renewable and clean [1], [2]. Since the photovoltaic effect was found, the semiconductor solar cells (SCs) have been widely used [3], [4]. With the efforts of scientists and engineers, the photoelectric conversion efficiency (PCE) of SC has progressed a lot [5]–[11]. The PCE of six-junction SCs has reached 47.1% [12]. The PCE of single-junction thin-film GaAs SC has amounted to 29.1% [13]. The PCE of Si heterojunction SC with intrinsic thin-layer has been reached 26.7% [14], which has been widely applied in civil power generation. Scientists are trying to achieve the theoretical efficiency limit of SC [6], [15]–[17].

Although the PCE of SC is soaring up, there are still some challenges to solve. As is known, the sun locates at a different azimuth in the daytime with the time change. So the SC cannot always work in the optimal condition because the PCE would vary with the angle of incident light [18]–[21]. Engineers constantly use an angel regulator to keep the panel perpendicular to the sunlight incident direction [22]. But this method does not fit in situations as assembling the SC on the object surface. Photonic crystal SC (PCSC) gives another choice to improve this. PC has been shown a capacity to manipulate the light. It could form a high-quality full-azimuth antireflection layer [23]–[25]. In this research, we have fabricated PCSCs with micro-scale PCs by ordinary ultra-violet lithography. Compared with the ordinary SC (OSC), the performance of PCSC is better and less sensitive to the incident light angle.

II. Experimental Details

In this work, GaAs-based SCs wafers were grown on lattice-matched GaAs (100) substrates with an electron concentration

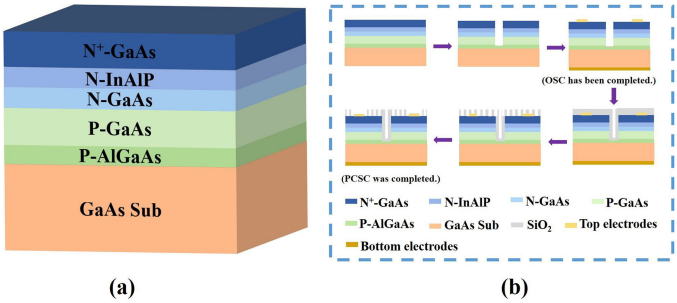

Fig. 1. (a) The epitaxial structure diagram of GaAs-based SC. (b) Preparation process steps of two samples.

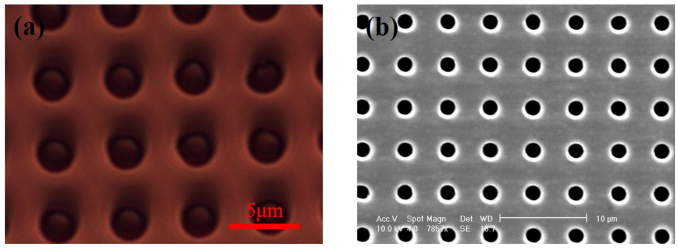

Fig. 2. (a) The microscope image of PCSC after development. (b) The SEM picture of PCSC after etching by RIE.

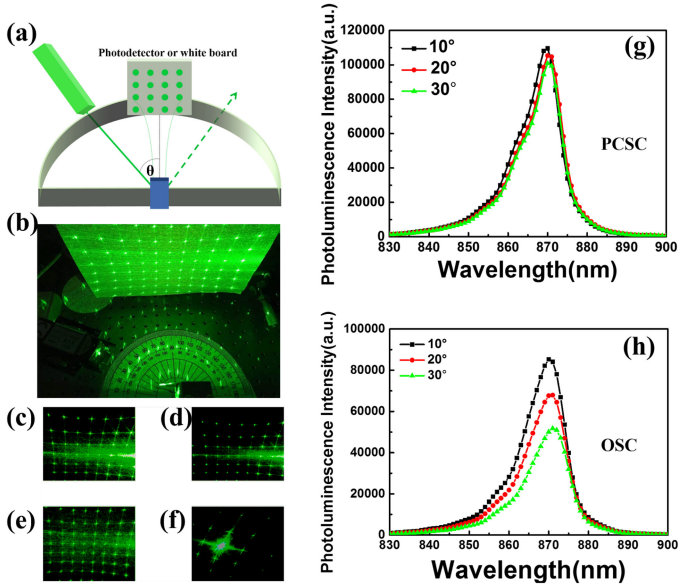

Fig. 3. (a) Schematic diagram of variable incident light angle testing. (b) Physical diagram of variable incident light angle testing. (c) Diffraction pattern of PCSC when the incident angle is 10°. (d) Diffraction pattern of PCSC when the incident angle is 20°. (e) Diffraction pattern of PCSC when the incident angle is 30°. (f) Main diffraction pattern of PCSC. (g) PL spectra of PCSC with different incident angles. (h) PL spectra of OSC with different incident angles.

of 5×10^{18} cm^{-3} by metal-organic chemical vapor deposition (MOCVD) system. The epi-layers comprise a 70-nm p-type AlGaAs layer, followed by a 3-μm p-type GaAs layer. Then a 100-nm n-type GaAs layer and a 30-nm InAlP window layer were grown. Finally, a 600-nm n-type GaAs contact layer was stacked on. The epitaxial structure diagram shows in Fig. 1(a). Ordinary GaAs-based SCs and GaAs-based SCs with two dimensional (2D) surface PC were fabricated as following steps, shown in Fig. 1(b). These 5 mm $\times$ 6 mm SC mesas were first formed by chemical etching after overlay photolithography. As for OSC, Ti/Au bottom electrodes and Ni/AuGe/Ni/Au top electrodes were then deposited by electron beam evaporation (EBE), followed by a rapid thermal annealing (RTA) process at 400°C in N_2 ambient to improve the ohmic contact property. For PCSC, a 300-nm SiO_2 was deposited on the top of OSC by plasma-enhanced chemical vapor deposition (PECVD). The 2D dot array was then made by standard UV lithography, followed by plasma reactive ion etching (RIE) with CF_4 and O_2. Next, the top electrodes were exposed by UV lithography and etched by RIE. Thus, all the required samples were prepared.

Next, we use a microscope and field-emission scanning electron microscope (SEM) (Hitachi S-4800) to measure the surface morphology and provide 10 kV high voltage to the electron gun. Furthermore, we also took a grating spectrometer to measure the photoluminescence (PL) of all samples. Meantime, we took a camera to record the diffraction pattern of PCSC. To measure the electronic properties of SCs, we took Keithley 4200 with the simulated sunlight.

III. Results

Microscope and SEM were used to study the surface morphology PCSC. Fig. 2(a) shows the photoresist pattern after the lithography process. It shows that the hole diameter is 2 μm and the pattern pitch is 5 μm. In this step, we use the AZ6130 photoresist and the MJB-3 lithography equipment. Fig. 2(b) shows the SEM image of PCSC, and it demonstrates that the 2D pattern had transferred to the SiO_2 completely. We use the model of Plasma 80 RIE equipment in which the RF power is 150 W for 8min with CF_4: O_2 (50:5) in this process.

Fig. 3 shows the PL spectra and the diffraction pattern variation with the azimuth of incident light. A 532 nm laser beam is emitted from the laser to excite the samples. We can see from Fig. 3(a) that the diffraction pattern projects on the whiteboard right above the sample. A grating spectrometer is also used to collect the photoluminescence signal in the normal direction. In the testing process, the laser moves around the sample to various incident angels. Fig. 3(b) shows the picture of the system framework when collecting the diffraction pattern. Fig. 3(c)$\sim$3(e) shows the diffraction pattern in the normal direction of PCSC when the incident angles are 10°, 20°, and 30°. We can see that the diffraction pattern does not change much with the incident angle. Diffractive spot comes from the modulation effect of PC on light. Due to the existence of photon gap, light can only propagate in the direction perpendicular to the surface of the epitaxial plate, and most of the light will come out of the hole, thus forming the regular arrangement of dot matrix pattern shape. The most bright spot in Fig. 3(c) and Fig. 3(d) is in the reflection path, confirmed in Fig. 3(f) by rotating the whiteboard to the reflection direction. And the single light spot intensity does not change too much by testing the output power. Fig. 3(g) and 3(h) show the PL spectra of samples. As we can see from Fig. 3(g), the PL intensity of PCSC does not change much with the incident light angle varying. When the incident light angle is 30°, the PL intensity is only 8% less than that of 10°. But for OSC, when the incident light angle is 30°, the PL intensity is 39% less than that of 10°. So the PC's ability to manipulate the light can make the SC less sensitive to the incident angle. A certain angle of incident light can be decomposed into vertical and parallel in the direction of the sample surface, and photonic

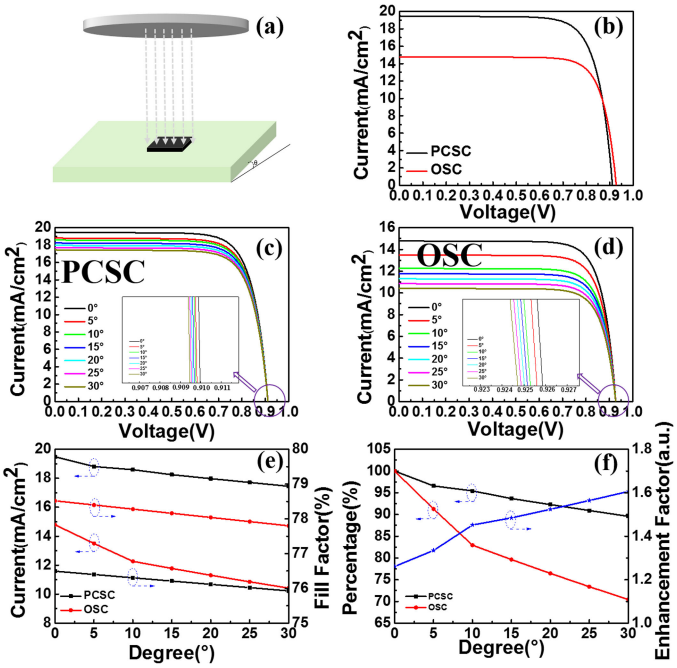

Fig. 4. (a) Schematic diagram of J-V curves testing. (b) J-V curves of two samples under the condition that incident angle is 0. (c) The changes of J-V curves with the angle of incident light of PCSC. (d) The changes of J-V curves with the angle of incident light of OSC. (e) The change of short circuit current and FF with angle and the ratio after the change of angle. (f) the change percentage of PCE after the change of angle.

bandgap of PC can inhibit the spread of light, making it in parallel to the direction of the surface of the sample light cannot escape from the side. Light can only choose the vertical direction to escape, which can ensure the most light incident to the sample inside, which is good for light absorptions. The reflected light, in addition to the reflectivity of the surface, also contains a certain vertical component. PL testing is a good and efficient non-destructive way of measuring the luminescence condition, which comprise of the absorption, spontaneous emission and light extraction processes. Solar cells pay more attention to the absorption of photons, so further investigation is needed.

Electronic properties of SCs are displayed in Fig. 4. J-V curves were obtained by Keithley 4200 with the solar simulator. Fig. 4(a) shows the schematic diagram of the J-V curve test. The angle of the incident light to the SC was adjusted by rotating the sample table. Fig. 4(b) shows the J-V curves of OSC and PCSC under the vertical illumination. The short current of PCSC is 32% higher than it of OSC due to more light absorption with the PC. But the open voltage (910 mV) and the fill factor (FF) (76.5%) of PCSC decrease comparing with OSC (926 mV, 78.52%), which can be explained by the reason that the SiO_2 deposited on the SC surface by PECVD at 380°C could deteriorate the ohmic contact and increase the series resistance. Fig. 4(c) and 4(d) respectively show the J-V curve variation with the incident angle of PCSC and OSC and the open circuit voltage varies very little. The light source in this experiment is not the standard AM1.0 simulated solar light, and the short-circuit current density is converted by combining the area of the device. The actual short-circuit current value is small, so the change of short-circuit current will not cause obvious change of open-circuit voltage. We can see that with the incident angle increasing, the short current of both samples decreases. Fig. 4(e) shows the short-circuit current and the FF variation with the angle. We can see that the short circuit current of OSC decreased more rapidly than it of PCSC. The gradient of the short circuit current decreasing for both OSC and PCSC gets more gentle with the incident angle rise. The short circuit current reduced 12% and 29.5%, corresponding to PCSC and OSC when the angle rose to 30° due to the reduction of the effective light absorption area and the increase of the reflection. For OSC, with the change of incident light angle, the effective receiving area of the device will decrease, so the short-circuit current will decrease rapidly. As for the PCSC, although the effective receiving area of the device decreases with the change of incident light angle too, most of the incident light still choose the propagation path perpendicular to the sample surface due to the PCs' light regulation effect, so the light intensity entering the sample has little change. Therefore, the short circuit current is not much reduced. And we can see that the FF decreasing gradient for SC and PCSC are almost the same. Fig. 4(f) shows and the decreasing percentage of PCE with the incident angle. The PCE of OSC went down more rapidly than it of PCSC, which corresponds to the change of the short-circuit current. Moreover, the PCE dropping gradient of PCSC became more flatten with the incident angle increasing. The PCE of PCSC and OSC reduced by 11.5% and 31.2%, respectively, when the incident angle rotated to 30°. Fig. 4(f) also shows the ratio of PCE between PCSC and OSC, which is defined as an enhancement factor. We can see that the enhancement factor of the PCE of PCSC to that of OSC increases from 1.26 to 1.6 as the incident angle rises to 30° from 0°, showing that PC plays a more and more indispensable role in light manipulation. PCSC benefits from manipulating the light, so its PCE is less sensitive to the incident angle. Furthermore, both the short-circuit current and PCE are improved. So PC can improve the static performance (the angle of incident light does not change) and improve the dynamic performance (the angle of incident light varies with time).

IV. Conclusion

In conclusion, high-performance GaAs-based PCSC was fabricated by the ordinary ultraviolet lithograph combined with RIE. Microscope and SEM measurements show the surface pictures of PCSC in the preparation process. PL testing shows that the intensity of PCSC and OSC changes with the incident light angle. When the incident light angle rises to 30°, the PL intensity is only 8% less than that of the incident light angle staying at 10°. But for OSC, the PL intensity reduced by 39%. Diffraction patterns that almost did not change in the normal direction of PCSC when the incident angles are 10°, 20°, or 30° respectively, were collected. For electrical properties, the short current of PCSC is improved by 32% compared with OSC. But the open voltage and the FF have decreased comparing with OSC because of the high-temperature process in PECVD. The short circuit current reduced by 12% and 29.5%, corresponding to PCSC and OSC when the angle rose to 30°. The change of FF of SC and PCSC is nearly the same. But the PCE reduced by 11.5% and 31.2%, corresponding to PCSC and OSC when the angle rotated to 30°. The enhancement factor of the PCE of PCSC to that of OSC increases from 1.26 to 1.6 as the incident angle rises to 30° from 0°, showing that PC plays a more and more indispensable role in light manipulation. The introduction of PC can help us design more optoelectronic devices with better performance.

REFERENCES

[1] N. Kannan and D. Vakeesan, "Solar energy for future world: - A review," *Renewable Sustain. Energy Rev.*, vol. 62, pp. 1092–1105, 2016.

[2] E. Kabir, P. Kumar, S. Kumar, A. A. Adelodun, and K. Kim, "Solar energy: Potential and future prospects," *Renewable Sustain. Energy Rev.*, vol. 82, pp. 894–900 2018.

[3] M. A. Green, "Photovoltaic principles," *Physica E Low-Dimensional Syst. Nanostructures*, vol. 14, pp. 11–17, 2002.

[4] R. Paul, "The photovohaic effect and its utilization," *Sol. Energy*, vol. 4, pp. 8–18, 1959.

[5] J. Xiao *et al.*, "Paths to light trapping in thin film GaAs solar cells," *Opt. Exp.*, vol. 26, 2018, Art. no. A341.

[6] T. Liu, K. Chen, Q. Hu, R. Zhu, and Q. Gong, "Inverted perovskite solar cells: Progresses and perspectives," *Adv. Energy Mater*, vol. 6, 2016, Art. no. 1600457.

[7] N. D. Gupta and V. Janyani, "Efficiency enhancement in the thin film GaAs solar cell using photonic crystal as a back reflector," in *Proc. Workshop Recent Adv. Photon.*, 2013, pp. 1–2.

[8] J. G. Mutitu *et al.*, "Thin film solar cell design based on photonic crystal and diffractive grating structures," *Opt. Exp.*, vol. 16, pp. 15238–15248, 2008.

[9] M. Yamaguchi, T. Takamoto, K. Araki, and N. Ekins-Daukes, "Multi-junction III–V solar cells: Current status and future potential," *Sol. Energy*, vol. 79, pp. 78–85, 2005.

[10] A. V. Shah *et al.*, "Thin-film silicon solar cell technology," *Prog. Photovolt.: Res. Appl.*, vol. 12, pp. 113–142, 2004.

[11] M. Yamaguchi, "III–V compound multi-junction solar cells: Present and future," *Sol. Energy Mater. Sol. Cells*, vol. 75, pp. 261–269, 2003.

[12] J. F. Geisz *et al.*, "Building a six-junction inverted metamorphic concentrator solar cell," *IEEE J. Photovolt,*, vol. 8, no. 2, pp. 626–632, Mar. 2018.

[13] B. M. H. N. Kayes, "27.6% conversion efficiency, a new record for single-junction solar cells under 1 sun illumination," in *Proc. Photovoltaic Specialists Conf.*, 2011, pp. 000004–000008.

[14] K. Yoshikawa *et al.*, "Silicon heterojunction solar cell with interdigitated back contacts for a photoconversion efficiency over 26," *Nature Energy*, vol. 2, 2017, Art. no. 17032.

[15] Y. Marouf, L. Dehimi, F. Bouzid, F. Pezzimenti, and F. G. D. Corte, "Theoretical design and performance of inx Ga1- xN single junction solar cell," *Optik*, vol. 163, pp. 22–32, 2018.

[16] Z. He *et al.*, "Single-junction polymer solar cells with high efficiency and photovoltage," *Nature Photon.,*, vol. 9, pp. 174–179, 2015.

[17] C. Hsu, J. Wu, Y. Lu, D. J. Flood, A. R. Barron, and L. Chen, "Fabrication and characteristics of black silicon for solar cell applications: An overview," *Mater. Sci. Semicond. Process.*, vol. 25, pp. 2–17, 2014.

[18] A. Meyer and H. Ade, "The effect of angle of incidence on the optical field distribution within thin film organic solar cells," *J. Appl. Phys.*, vol. 106, 2009, Art. no. 113101.

[19] H. Heidarzadeh, "Incident light management in a thin silicon solar cell using a two-dimensional grating according a Gaussian distribution," *Sol. Energy*, vol. 189, pp. 457–463, 2019.

[20] Z. H. Lu and Q. Yao, "Energy analysis of silicon solar cell modules based on an optical model for arbitrary layers," *Sol. Energy,*, vol. 81, pp. 636–647, 2007.

[21] M. R. Lewis *et al.*, "Angular dependence of textured bifacial silicon heterojunction solar cells for high latitudes," in *Proc. IEEE 46th Photovoltaic Specialists Conf.*, 2019, pp. 1919–1923.

[22] T. Yagi, Y. Uraoka, and T. Fuyuki, "Ray-trace simulation of light trapping in silicon solar cell with texture structures," *Sol. Energy Mater. Sol. Cells*, vol. 90, pp. 2647–2656, 2006.

[23] J. M. Delgado-Sanchez and I. Lillo-Bravo, "Angular dependence of photonic crystal coupled to photovoltaic solar cell," *Appl. Sci.*, vol. 10, 2020, Art. no. 1574.

[24] Z. Liu *et al.*, "Improving efficiency and stability of colorful perovskite solar cells with two-dimensional photonic crystals," *Nanoscale*, vol. 12, pp. 8425–8431, 2020.

[25] N. D. Gupta and V. Janyani, "Design and analysis of light trapping in thin film GaAs solar cells using 2-D photonic crystal structures at front surface," *IEEE J. Quantum Electron.*, vol. 53, no. 2, pp. 1–9, Apr. 2017.